中國機械工程學刊第四十五卷第四期第 345~354 頁(民國一百一十三年)
Journal of the Chinese Society of Mechanical Engineers, Vol.45, No.4, pp345~354 (2024)

Adaptive Fractional Order PID Controller for Angle Tracking in Steer-By-Wire System

Cong-Cong Guo*, Chang-Shui Wu**and De-Guan He***

Keywords：SBW technology, angle-tracking-control, Improved particle swarm algorithm, FOPID controller.

ABSTRACT

To ensure fast and accurate angle tracking during car steering, reduce delay time, and improve the tracking performance of the Steer-by-Wire (SBW) system, a fractional order PID (FOPID) controller with feedforward compensation is designed. The PID controller is approximated using the Oustaloup approximation method, reducing the tuning dimension of FOPID. An improved particle swarm optimization (PSO) algorithm is utilized to dynamically adjust the four parameters of FOPID, thereby decreasing the optimization time of the algorithm. Finally, the Adaptive Inertia Weight Particle Swarm Optimization algorithm (AW-PSO), based on global search pattern, the Fixed Inertia Weight Particle Swarm Optimization algorithm (F-PSO), based on variable neighborhood search pattern, and the Compressed Factor Particle Swarm Optimization algorithm (CF-PSO) are used as comparisons for simulation verification and bench test. The effectiveness of the proposed method is verified. The comparative results show that, in terms of computation time and accuracy, the optimization capability of the proposed method is significantly superior to the AW-PSO, F-PSO, and CF-PSO algorithms. Hence, the algorithm's computation accuracy and stability fully meet the requirements. The bench test results reveal that under step input, the delay time is about 0.2s, with a maximum overshoot of 1.57deg. Under sinusoidal input, the delay time is approximately 0.02s, the maximum steering speed is 0.70rad/s, and the maximum output torque of the steering motor is 2.27Nm. Based on experimental verification, it can be possible to conclude that this method enables better completion of the angle tracking control task for the SBW system and exhibits good robustness and tracking control performance

Paper Received August, 2023. Revised December, 2023. Accepted January, 2024. Author for Correspondence: Chang-Shui Wu. wuchangshui@sues.edu.cn

*** Associate Professor, Department of Mechanical Engineering, Shanghai University of Engineering Science, Shanghai, Shanghai 201620, China.*

** Graduate Student, Department of Mechanical Engineering, Shanghai University of Engineering Science, Shanghai, Shanghai 201620, China.*

**** R&D Supervisor, Department of R&D, Suzhou Hiro Automotive Parts Co, Suzhou, Suzhou 215300, China.*

INTRODUCTION

In the past 50 years, SBW technology has been established in the 1970s and has since developed to a mature stage. The SBW system can be independently controlled without driver operation, even without a steering wheel, and precise tracking control of the steering angle is an important technology for autonomous driving (JIN .2022). Achieving superior accuracy, low latency, and high stability in online steering angle tracking control is often challenging. Many domestic and foreign scholars have conducted extensive research on this. Xu et al. (2019) designed a FOPID controller, optimized its five parameters using genetic algorithms, and achieved better control performance than traditional PID controllers. However, it is a long delay and cannot provide good angle tracking accuracy under complex operating conditions. Zhang et al. (2021) designed a robust linear quadratic regulator with appropriate robustness and suitable for real-time control on low-cost MCUs, but accuracy remains difficult to guarantee. To address this issue, Zhang et al. (2022) proposed a dual-motor SBW control strategy for steering angle-tracking. It utilizes dual-motor synchronous control and angle tracking closed-loop control to handle the asynchronous response between the two steering actuator motors, which affects vehicle stability. The strategy also reduces angle synchronization error through current compensation feedback, greatly enhancing the reliability of the SBW system. Xu et al. (2022) introduced a generalized predictive control method based on Taylor approximation. This algorithm has a relatively simple structure and is easy to tune and implement. It achieves high performance in terms of angle tracking, fast response, and stability.

Sun et al. (2016) proposed an adaptive sliding mode (ASM) controller that treats tire-ground friction force and self-aligning torque as external disturbances.

The controller uses sliding mode control to handle parameter uncertainties and estimates the self-aligning torque coefficient through a self-adaptive torque estimation method. Experimental results demonstrate that the ASM controller maintains excellent robustness while ensuring good tracking accuracy. Yu et al. (2021) presented an angle tracking control method for the SBW system based on internal model control (IMC), with the addition of active disturbance rejection control (ADRC) in the IMC framework. The method dynamically estimates the self-aligning torque acting on the steering tie rod using an extended state observer (ESO). Simulation experiments show that this controller achieves good accuracy and robustness. In order to balance the stability and accuracy of the system, Shi et al. (2023) employed the model predictive control (MPC) method and designed an adaptive PI controller. A comparative experiment was conducted with a PI controller and a sliding mode controller on a steering test bench. The results showed that the three controllers had similar root mean square errors during sinusoidal steering cycle tests and complex steering conditions. Among them, MPC had the lowest error and achieved limited improvement, meeting the steering requirements of the SBW system. In addition to the aforementioned methods, real-time adjustments to the system can also be made using optimization algorithms. The particle swarm optimization algorithm, which has evolved and been optimized for several decades, is now well-established and widely applied in academia and industry. He et al. (2022) proposed an adaptive particle swarm optimization PI controller (PSAPI) that dynamically updates the PI parameters using the particle swarm optimization algorithm. A comparison was made with a PI controller, fuzzy PI controller (FPI), model predictive controller (MPC), and sliding mode predictive controller (SMPC) through bench experiments. The experimental results showed that PSAPI achieved better tracking performance.

A self-adaptive FOPID (Fractional Order Proportional Integral Derivative) controller with feedforward compensation was designed. The system was dynamically adjusted in real-time using an improved particle swarm optimization algorithm and feedforward compensation. To avoid falling into local optimality, the particle swarm algorithm employed a variable neighborhood search pattern, adaptive inertia weight, and compression factor method, which not only ensured the optimization capability but also reduced the system's time delay. In this paper, the proposed controller was validated in an autonomous driving scenario. The experimental results demonstrated that the controller significantly reduced the overshoot and delay time in steering angle tracking while ensuring accuracy requirements. It also exhibited good robustness. For complex steering conditions in automotive applications, the controller achieved excellent tracking performance and fully met the steering requirements of autonomous driving and driver assistance systems.

STEER-BY-WIRE SYSTEM

The steering system is a critical system to realize the driver's steering intention and control the vehicle's handling stability. Traditional automotive steering systems can be divided into two categories based on different steering energy sources: mechanical steering systems and power steering systems. Although traditional steering systems can effectively ensure that cars turn and drive according to the driver's intentions, due to their fixed or limited steering transmission ratios, the steering response characteristics of cars vary with vehicle speed. Therefore, drivers must compensate for the amplitude and phase changes of the car's steering characteristics to steer the car according to their wishes. However, this greatly affects the handling stability and driving comfort of the car. The wire controlled steering system eliminates the mechanical connection between the steering wheel and the steering wheel, completely breaking away from various limitations of traditional steering systems.

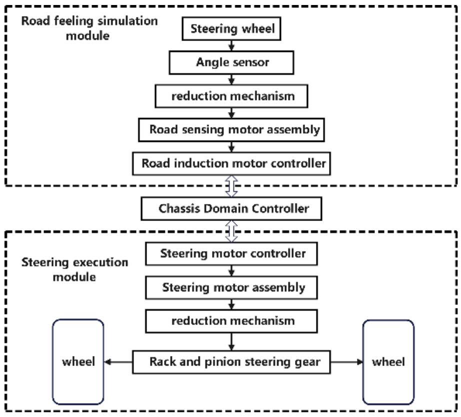

Fig.1 Structure diagram of wire controlled steering system

The driver's steering operation is only to input the steering wheel angle command to the vehicle. Under certain stable operating conditions, the controller determines a reasonable front wheel angle based on information such as the steering wheel angle and current vehicle status, and relevant control algorithms to achieve "just right" steering at the same time, Drivers need to know the information of the road surface. As there is no mechanical connection between the steering wheel and the steering wheel, "road feel" needs to be simulated and generated. Only with "road feel" can drivers achieve a "clear understanding" when turning. The steering-by-wire system can be designed with variable transmission ratios, which not only changes the steering characteristics but also greatly improves the vehicle's handling and stability, reduces the driver's handling burden, and improves the performance of the person vehicle closed-loop system. steer-by-wire technology is an important part of the chassis domain system, involving multiple areas. Its adjustable steering ratio greatly improves the handling stability of the vehicle. The key technologies in the steer-by-wire system include sensor technology, active steering technology, and fault-tolerant control technology. The key technology in active steering is angle control technology. The SBW system can compensate for wheel steering angles and adjust steering errors, thereby improving the lateral stability of the vehicle. (Zhang et al.,2021)

STEER-BY-WIRE SYSTEM ARCHITECTURE

The steer-by-wire system, as shown in Figure 1, consists of a chassis domain controller, a permanent magnet synchronous motor (PMSM), a motor electronic control unit (ECU), a ball screw mechanism, and other structures. PMSM is selected as the steering actuator motor for the SBW system, driven by the direct torque control method. This method has advantages such as simple algorithm and good torque response. Integrated permanent magnet synchronous motors are used as driving motors for SBW systems due to their advantages of simple structure, low processing and assembly costs, and better suitability for large-scale industrial production.

The steer-by-wire system allows steering operations without a driver or even a steering wheel ((Chen et al.,2022)). The angle command issued by the upper-level or autonomous driving domain controller is sent to the FOPID controller in the chassis domain controller. The controller calculates the required torque for the PMSM and sends it to the steering actuator motor ECU. The motor generates the torque and transmits it to the wheels through the mechanical structure, completing the steering operation.

STEERING DYNAMICS MODEL

Based on automotive dynamics, the differential equations for each component are established (Wei et al.,2021; Chen et al.,2019; Li et al.,2022).

Differential equation for the motion of the steering motor:

$$T_m = T_s p + I_m \ddot{\delta}_m + B_m \dot{\delta}_m . \tag{1}$$

Where T_m and T_{sp} represent the required torque of the steering actuator motor and the resistance torque of the small gear, respectively.

The differential equation for the motion of the small gear is:

$$T_{sp} = (F_u - F_l) r_{sp} + I_{sp} \ddot{\delta}_{sp} + B_{sp} \dot{\delta}_{sp} + \tau_{sp} , \tag{2}$$

$$(F_u - F_l) r_{lp} = T_{lp} + I_{lp} \ddot{\delta}_{lp} + B_{lp} \dot{\delta}_{lp} + \tau_{lp} , \tag{3}$$

$$T_{lp} = T_{bs} + I_{bs} \ddot{\delta}_{bs} + B_{bs} \dot{\delta}_{bs} + \tau_{bs} . \tag{4}$$

Where F_u , F_l , r_{sp} , T_{lp} , r_{lp} , T_{bs} represent the tension in the upper timing belt, tension in the lower timing belt, radius of the small gear, output torque of the large gear, radius of the large gear, and output torque of the ball screw, respectively.

The differential equation for the motion of the ball screw is:

$$T_{bs} \cdot \dot{\delta}_{bs} = \left(F_{th} + m_d \ddot{D} + B_d \dot{D} \right) \dot{D} . \tag{5}$$

Where F_{th}, D, m_d represent the tension in the tie rod, displacement of the tie rod, and mass of the tie rod, respectively.

The differential equation for the motion of the front wheels of the car is:

$$T_f - \tau_{ef} = I_f \ddot{\delta}_f + B_f \dot{\delta}_f + \tau_f . \tag{6}$$

Where T_f represents the output torque of the steering lever, and satisfies:

$$\tau_f = F_s \operatorname{sgn}\left(\dot{\delta}_f \right). \tag{7}$$

By combining the above equations, the differential equation for the motion of the steer-by-wire system can be obtained as:

$$I_{eq} \ddot{\delta}_f + B_{eq} \dot{\delta}_f + f_{eq} + \tau_{ef} = i_{steer} T_m . \tag{8}$$

Where I_{eq} , f_{eq} , B_{eq} , and τ_{ef} represent the equivalent moment of inertia, rotational friction torque, and viscous friction torque of the steering system, respectively. And I_{eq}, B_{eq}, i_{steer} satisfy the following relationship:

$$\begin{cases} I_{eq} = I_f + i_{screw}^2 i_{lever}^2 \cdot \\ \qquad (J_{lp} + I_{bs} + m_d / i_{screw}^2 + i_{pulley}^2 (\mathrm{I_m} + I_{sp})) \\ B_{eq} = B_f + i_{screw}^2 i_{lever}^2 \cdot \\ \qquad (B_{lp} + B_{bs} + B_d / i_{screw}^2 + i_{pully}^2 (B_\mathrm{m} + B_{sp})) . \\ f_{eq} = \tau_f + i_{srew} i_{lever} (i_{screw}^2 f_{sp} + f_{lp} + f_{bs}) \end{cases} \tag{9}$$

From equation (9), it can be seen that the required torque of the steering actuator motor is:

$$T_m = \frac{I_{eq} \ddot{\delta}_f + B_{eq} \dot{\delta}_f + f_{eq} + \tau_{ef}}{i_{steer}} . \tag{10}$$

DETERMINING THE SYSTEM GEAR RATIO

Compared to mechanical steering, the wire-controlled steering system utilizes a variable gear ratio, which allows for the design of different gear ratios based on varying vehicle speed and steering angle requirements. In order to achieve a neutral steering condition as much as possible, corresponding gear ratios are designed. For low-speed driving, where a large steering input is required during turns, the system's steering sensitivity should be increased by using a smaller gear ratio. However, to prevent the steering from being overly sensitive, a minimum value should be set. On the other hand, for high-speed driving, in order to enhance handling stability and minimize the negative effects of driver misoperation, a larger gear ratio should be employed. However, care should be taken to avoid excessively large gear ratios, which may result in delayed steering response during overtaking maneuvers and other driving conditions. Therefore, an appropriate value should be selected as the maximum gear ratio.

The gear ratios designed in this paper are as follows:

1) For vehicle speeds of 0 ~ 20 km/h: a minimum gear ratio of 6 is set to enhance steering sensitivity.
2) For vehicle speeds of 20 ~ 90 km/h: the gear ratio is designed using a method that maintains a constant steady-state yaw angular velocity gain.
3) For vehicle speeds of 90 ~ 120 km/h: the gear ratio is designed using fuzzy control to reduce steering sensitivity during high-speed driving.
4) For vehicle speeds above 120 km/h: a maximum gear ratio of 25 is set to lower steering sensitivity and enhance handling stability.

ADAPTIVE FOPID FEEDFORWARD COMPENSATION CONTROLLER

Integer-order PID controllers have been widely used in process control for decades due to their simple design and good performance. In FOPID controllers, in addition to the Kp, Ki, and Kd parameters of the integer-order PID controller, two additional parameters, namely the fractional-order integral λ and fractional-order derivative μ, are introduced. Therefore, compared to integer-order PID controllers, FOPID controllers are more flexible, accurate, and can achieve better robustness (Yin et al.,2019; Liu et al.,2021; Pietruch et al.,2022; Xie et al.,2023; Cheng et al.,2023). The relationship between the two is shown in Figure 2.

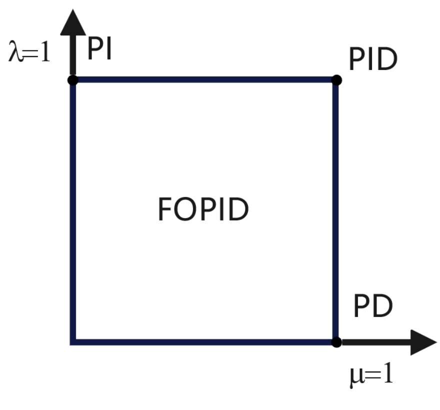

Fig.2 Relationship between FOPID and PID

The generalized PID (FOPID) transfer function is defined as follows:

$$G_C(s) = K_p + \frac{K_i}{s^{\lambda}} + K_d s^{\mu}. \tag{11}$$

When λ=1 and μ=1, Equation 10 represents an integer-order PID controller, that is:

$$G_C(s) = K_p + \frac{K_i}{s} + K_d s. \tag{12}$$

By approximating the PID using the Oustaloup algorithm, the dimensionality of FOPID is reduced. Furthermore, based on the method of feedforward compensation, the improved particle swarm algorithm is used to optimize the FOPID parameters in real time. The controller structure is shown in Figure 3.

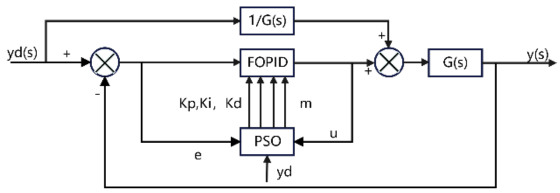

Fig.3 Structure diagram of FOPID controller

FOPID CONTROLLER

The designed feedforward compensation output is given by:

$$u_f(s) = y_d(s)\frac{1}{G(s)}. \tag{13}$$

The total output of the controller is then:

$$u(t) = u_p(t) + u_f(t). \tag{14}$$

The rational function approximation of the fractional calculus operator's transfer function under the Oustaloup filter is:

$$H(s) = \frac{1}{(\omega_c)^m}\frac{\prod_{i=1}^{N}\left(1+\frac{s}{Z_i}\right)}{\prod_{i=1}^{N}\left(1+\frac{s}{p_i}\right)}. \tag{15}$$

Where, for i = 1, 2, ..., N, the zero Z_i, pole p_i, and approximation error ε are given respectively:

$$\begin{cases} p_1 = \omega_c 10^{\alpha}, Z_1 = p_1 10^{\rho m} & ,i=1 \\ p_i = 10^{\rho} p_{i-1}, Z_i = p_i 10^{\rho m} & ,i \geqslant 1 \\ \varepsilon = \dfrac{m(1-m)}{(2N+1-m)}\left[\log\left(\dfrac{\omega_M}{\omega_c}\right)\right] \end{cases}. \tag{16}$$

m is the order of the approximated generalized fractional calculus, and A, as well as the other approximation parameters in Equation 16, are:

$$\begin{cases} \rho = \dfrac{2\varepsilon}{(1-m)m}, \quad \alpha = \dfrac{\varepsilon}{m} \\ \omega_C = \gamma\omega_L\,(0.001 \leqslant \gamma \leqslant 10000) \\ \omega_M = \theta\omega_H\,(10 \leqslant \theta \leqslant 10000) \end{cases}. \tag{17}$$

The approximate transfer function of the FOPID is given by:

$$C(s) = (K_i)^m\left(\frac{\left(1+\frac{s}{\lambda_1}\right)\left(1+\frac{s}{\lambda_2}\right)}{s}\right)^m. \tag{18}$$

$\lambda_1 < \lambda_2$,and:

$$\begin{cases} \lambda_1 = \dfrac{K_p - \sqrt{K_p^2 - 4K_d K_i}}{2K_d} \\ \lambda_2 = \dfrac{K_p + \sqrt{K_p^2 - 4K_d K_i}}{2K_d} \end{cases}. \tag{19}$$

In conclusion, the rational function approximation of the FOPID transfer function can be obtained as follows:

$$\begin{cases} D(s) = \left[\dfrac{1}{(\omega_{c_1})^m} \dfrac{\prod_{i=1}^{N_1} \left(1 + \frac{s}{Z_i}\right)}{\prod_{i=1}^{N_1} \left(1 + \frac{s}{p_i}\right)} \right] \\ E(s) = \left[\dfrac{1}{(\omega_{c_2})^m} \dfrac{\prod_{i=1}^{N_2} \left(1 + \frac{s}{Z_i}\right)}{\prod_{i=1}^{N_2} \left(1 + \frac{s}{p_i}\right)} \right] \\ C(s) = D(s) \left(\dfrac{K_i}{\lambda_2} \right)^m \end{cases}. \tag{20}$$

PARTICLE SWARM ALGORITHM OPTIMIZATION

To improve the optimization capability of the algorithm and avoid getting stuck in local optima, an adaptive neighborhood search mode is employed in this paper. In addition to the global mode where all particles are considered neighborhood particles, the neighborhood mode divides particles into multiple subgroups. Each particle only considers the particles within its neighborhood range as its neighborhood particles. When the fitness change rate reaches a critical value, the neighborhood range expands, and the population transitions from the neighborhood mode to the global mode. If the change rate is below the critical value, it reverts back to the neighborhood mode. The fitness function is defined as follows:

$$J = \int t|e(t)|dt. \tag{21}$$

Defined in a 4-dimensional search space A, there are 100 particles. The position and update velocity of the particles after the i-th (i=1,2,...,20) iteration are defined as:

$$\begin{cases} x_i^k = [x_{K_p}^k, x_{K_i}^k, x_{K_d}^k, x_m^k] \\ v_i^k = [v_{K_p}^k, v_{K_i}^k, v_{K_d}^k, v_m^k] \end{cases}. \tag{22}$$

The corresponding update formula is as follows:

$$\begin{cases} sy = c_1 r_1 (B_{Pbest}{}_i^k - x_i^k) \\ gr = c_2 r_2 (B_{Gbest}{}_d^k - x_d^k) \\ v_i^{k+1} = \Phi[\omega v_i^k + sy + gr] \\ \quad x_{id}^{k+1} = x_i^k + v_i^{k+1} \end{cases}. \tag{23}$$

C_1, C_2, i, ω, B_{Pbest}, B_{Gbest}, Φ refer to the self-learning factor, social learning factor, algorithm iteration count, inertia weight, individual best position, neighborhood best position, and compression factor, respectively. The adaptive inertia weight is defined as:

1) $f(x_i^k) \geqslant f_{average}^k$:

$$\omega_i^k = \omega_{\min} + (\omega_{\max} - \omega_{\min}) \frac{f_{\max}^k - f(x_i^k)}{f_{\max}^k - f_{average}^k}, \tag{24}$$

2) $f(x_i^k) < f_{average}^k$:

$$\omega_i^k = \omega_{\max}. \tag{25}$$

$\omega_{\max}$, $\omega_{\min}$, $f_{average}^k$, $f_{\max}^k$, $f_{\min}^k$ represent the upper and lower bounds of the inertia weight, as well as the average fitness and the maximum and minimum fitness of all particles in the k-th iteration. The compression factor is calculated using the following formula:

$$C_1 = C_2 = 2.05$$
$$C = C_1 + C_2 = 4.1$$
$$\Phi = \frac{2}{\left|\left(2 - C - \sqrt{C^2 - 4C}\right)\right|} \tag{26}$$

From equation (26), it can be inferred that the PID parameters should satisfy:

$$\sqrt{K_p^2 - 4K_d K_i} > 0. \tag{27}$$

From equation (27), it can be inferred that the range of values for K_p, K_i, and K_d is:

$$\begin{cases} K_i \in [0, 20] \\ K_d \in [0, 20] \\ K_p \in \left[2\sqrt{K_i K_d}, 100\right] \end{cases}. \tag{28}$$

EXPERIMENTAL VERIFICATION

This chapter will be divided into three parts to examine the designed adaptive FOPID controller in this paper. Firstly, a comparison test will be conducted with similar algorithms using test functions, along with measuring the computational time of the particle swarm algorithm. Secondly, a dynamic model will be established to perform joint simulations for comparing the controller with similar ones, evaluating the optimization level of the algorithm, and as well as assessing factors such as time delay and overshoot. Finally, the program will be burned onto the experimental platform to validate the system's response to upper-level steering commands under the influence of a spring load.

COMPARISON TEST OF PARTICLE SWARM OPTIMIZATION ALGORITHM

The four test functions (as shown in Table 1) are used to compare the particle swarm optimization (ZPSO) algorithm in the “ARTICLE SWARM ALGORITHM OPTIZATION” section with similar Particle swarm optimization algorithms. The comparable PSO algorithms include, Adaptive Inertia Weight Particle Swarm Optimization (AW-PSO) based on global search mode (Mezura et al.,2011), Fixed Inertia Weight Particle Swarm Optimization (F-PSO) based on variable neighborhood search mode, and Particle Swarm Optimization using the Compression Factor method (CF-PSO) (Wei et al.,2022): with the values n=30, $C_1=C_2$=2.05, $\omega_1=\omega_{\max}$=0.9, $\omega_{\min}$=0.4. To ensure both sufficient accuracy and shorter latency, the maximum number of iterations is set to 20. After ten measurements and calculations of the average values, the results are presented in Table 2.

Table 1. Comparison test function

Function Name	Function Expression	Range	Theory Extreme Value	Error Target
Sphere	$f(x)=\sum_{i=1}^{n} x_i^2$	[-100, 100] ^{n}	0	0.01
Rosenbrock	$f(x)=\sum_{i=1}^{n-1} 100(x_{i+1}-x_i^2)^2+(x_i-1)^2$	[-30, 30] ^{n}	0	100
Rastrigin	$f(x)=\sum_{i=1}^{n}(x_i^2-10\cos(2\pi x_i)+10)$	[-5.12, 5.12] ^{n}	0	100
Griewank	$\frac{1}{4000}\sum_{i=1}^{n} x_i^2-\prod_{i=1}^{n}\cos\left(\frac{x_i}{\sqrt{i}}\right)+1$	[-600, 600] ^{n}	0	0.1

Table 2. Comparison of test results

Function Name	APSO	BPSO	CPSO	ZPSO
Sphere	1.8595×10^(-7)	1.2777×10^(-7)	2.6777×10^(-7)	8.8493×10^(-8)
Rosenbrock	0.2678	0.0901	0.5428	0.0412
Rastrigin	61.3827	41.9674	72.6319	37.8263
Griewank	0.0271	0.0099	0.0369	0.0051

Table 3. Description of relevant parameters

Parameters Name	Parameter Description	Unit
δ_m	Angle of steering motor	rad
δ_{sp}	Angle of small pulley	rad
δ_{lp}	Angle of large pulley	rad
δ_{bs}	Angle of ball screw	rad
δ_f	Angle of front wheel	rad
B_m	Viscous friction of steer motor shaft	N•m•s
B_{sp}	Viscous friction of small pulley	N•m•s
B_{lp}	Viscous friction of large pulley	N•m•s
B_{bs}	Viscous friction of ball screw	N•m•s
B_d	Viscous friction of drag rod	N•m•s
B_f	Viscous friction of front wheel	N•m•s
I_m	Inertia of motor shaft	kg•m^2
I_{sp}	Inertia of small pulley	kg•m^2
I_{lp}	Inertia of large pulley	kg•m^2
I_{bs}	Inertia of ball screw	kg•m^2
I_f	Inertia of front wheel	kg•m^2
τ_{sp}	Friction torque of small pulley	N•m
τ_{lp}	Friction torque of large pulley	N•m
τ_{bs}	Friction torque of ball screw	N•m
τ_{ef}	Torque imposing on front wheels	N•m
C_f	Tire lateral stiffness of front wheel	N•m /rad
C_r	Tire lateral stiffness of rear wheel	N•m /rad
M_v	Gross vehicle weight	kg
l_f	Length from front axis to gravity center	m
l_r	Length from rear axis to gravity center	m
l_L	Length of the tire footprint	m
I_{eq}	the equivalent moment of inertia	kg•m^2
f_{eq}	the equivalent moment of rotational friction torque	N•m
B_{eq}	the equivalent moment of viscous friction torque	N•m
τ_{eq}	the equivalent moment of steering system	N•m
D	displacement of the tie rod	m
F_u	the tension in the upper timing belt	
F_l	tension in the lower timing belt	
r_{sp}	radius of the small gear	
T_{lp}	output torque of the large gear	
r_{lp}	radius of the large gear	
T_{bs}	output torque of the ball screw	

The results show that the particle swarm algorithm proposed in 3.2 exhibits a reduction in calculation errors of 30.7% to 66.9% compared to APSO, BPSO, and CPSO on the Sphere test function. For the Rosenbrock test function, the calculation errors decrease by 54.3% to 92%. Similarly, for the Rastrigin test function, the errors decrease by 9.8% to 47.9%, and for the Griewank test function, the errors decrease by 48.5% to 86.2%. Consequently, it can be concluded that the particle swarm algorithm proposed in 3.2 demonstrates significantly superior optimization capabilities compared to the other three algorithms. Therefore, this algorithm exhibits greater precision and stability in meeting the requirements.

EPS BENCH TEST

To validate angle tracking control in autonomous driving scenarios, an Electric Power Steering (EPS) bench test is conducted for angle control without a steering wheel. The bench test setup, as shown in Figure 4, includes the integration of angle control and motor drive programs within the Electronic Control Unit (ECU). The bench test consists of a steering wheel assembly, steering actuator assembly, host computer, 12V DC power supply, and a spring load. The maximum spring load during rack travel is 20 kN. Communication is established between CANalyzer and the ECU, with CANalyzer sending steering angle commands to the ECU. The ECU calculates the required motor torque and controls it directly to the steering actuator assembly, thus achieving front-wheel angle control. This paper analyzes the steering performance in autonomous driving scenarios from four aspects: time delay, overshoot, accuracy, and rotational speed (Xie et al.,2022; Shi et al.,2022).

Fig.4 EPS Test bench

CASE I: STEP RESPONSE

Set a continuous step signal with a step value of A in CANalyzer, and record the angle value, motor torque, and steering speed in CANape.

As shown in Figure 5-7, significant fluctuations occur around 9.2 seconds. At this point, the system experiences a brief delay of approximately 0.2 seconds and an overshoot of around 10 degrees after receiving a step input steering angle command of 40 degrees. It then re-enters a steady state, quickly reducing the tracking error. The steady-state error is approximately 2 degrees, as shown in Figure 10. At this time, the steering speed reaches 0.94 rad/s, and the motor torque is 1 Nm. The torque exhibits minimal fluctuations. Even under high-speed command inputs, the system is still capable of quickly reaching a steady state.

During the testing process, The maximum overshoot is 1.57 degrees, and the maximum steering speed is 1.17rad/s. The maximum output torque of the steering motor is 1.66Nm. Therefore, it can be concluded that the system can quickly reach the target angle after receiving the angle command and can maintain the steering wheel angle error at around 1 degree in steady-state conditions.

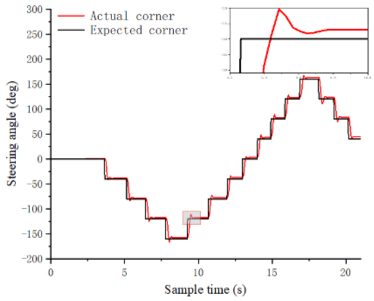

Fig.5 Steer angle of EPS bench

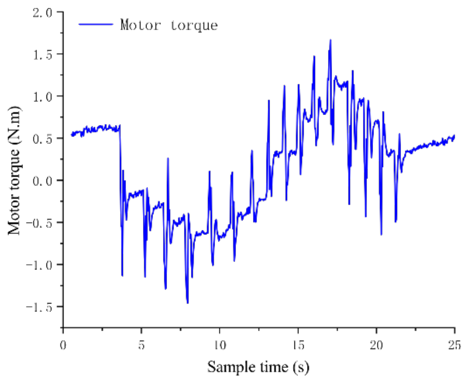

Fig.6 Motor torque of EPS bench

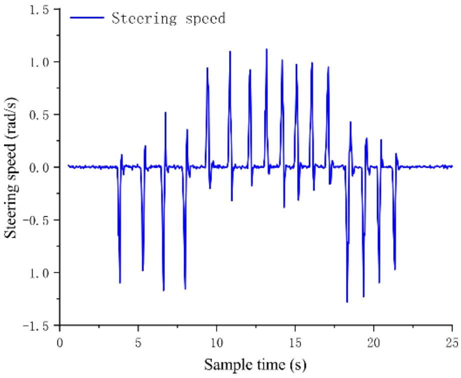

Fig.7 Steering speed of EPS bench

CASE II: SINUSOIDAL RESPONSE

In CANalyzer, the desired steering angle is set to 300 with a period of 10 seconds using a sinusoidal waveform. The steering angle command is sent to the ECU through CANalyzer, and the steering angle, motor torque, and steering speed are recorded in CANape.

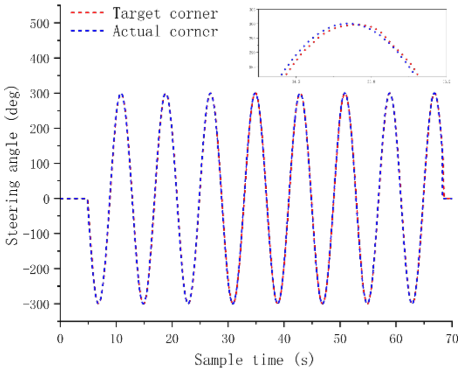

Fig.8 Comparison of steering angles under sinusoidal signal input of EPS bench

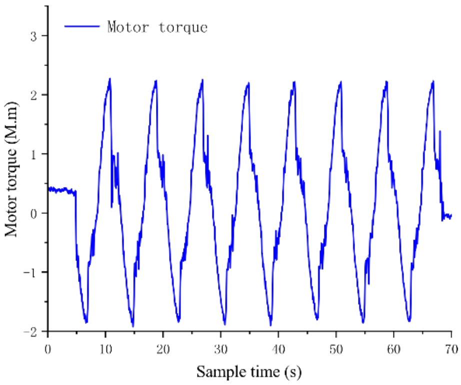

Fig.9 Motor torque under sinusoidal signal input of EPS bench

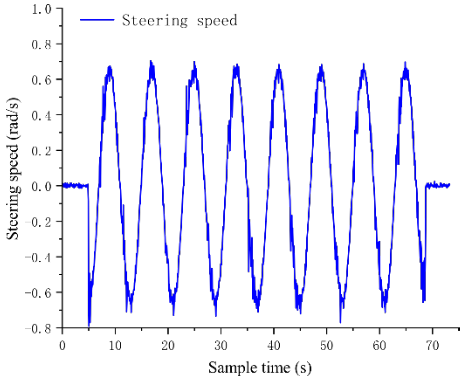

Fig.10 Steering speed under sinusoidal signal input

As shown in Figures 8 to 10, under the given sinusoidal signal input, the system demonstrates better tracking control performance compared to a step input. The delay time is approximately 0.02 seconds, the maximum steering speed is 0.70rad/s, and the maximum output torque of the steering motor is 2.27Nm. The system only produces larger noise points at the beginning and end of the angle control, but they are still within a reasonable range. Therefore, it can be concluded that under these test conditions, the system can achieve good angle tracking control performance.

CONCLUSIONS

This study investigates the performance of the adaptive FOPID controller in angle tracking control of steer-by-wire systems. The following key findings are presented:

1) By comparing four test functions mentioned in reference with three other similar optimization algorithms, the proposed particle swarm optimization (PSO) algorithm demonstrates significantly superior optimization capability compared to AW-PSO, F-PSO, and CF-PSO. The errors are within the reasonable range specified in reference, indicating the stability and optimization ability of the algorithm.

2) Through simulation comparisons with similar controllers, the designed controller in this study achieves a reduction of 73.67% and 7.36% in maximum tracking errors, as well as a reduction of 78.79% and 50% in average tracking errors, respectively. The time delay is shortened by 20.71% and 13.29%. These improvements in time delay, control accuracy, and robustness are evident compared to other similar controllers.

3) The overall performance of the controller is tested through EPS bench experiments. The results demonstrate that the ZFOPID controller exhibits strong robustness, shorter time delay, and good tracking control performance.

The designed controller in this study demonstrates favorable control effects in terms of time delay, overshoot, and control errors. However, when the steering angle changes rapidly (1 rad/s), significant overshoot may occur due to factors such as inertia. Nonetheless, this overshoot remains within a reasonable range. Future work will focus on addressing this issue to further improve the controller's performance.

REFERENCES

Chen, L.B., "Research on Adaptive Terminal Sliding Mode Control of a Wire Control Steering System Considering Vehicle Lateral Stability," M.S. Thesis, *Xihua University*, Chengdu, Sichuan (2022).

Chen, X. B., Q. L. Bao, and B. Zhang. "Research on 4wis Electric Vehicle Path Tracking Control Based on Adaptive Fuzzy Pid Algorithm." ;,Proc., *Proceedings of the 38th Chinese Control Conference (Ccc)* (2019): 6753-60.

Su, C. R., H. H. Li, B. J. Qiao, and X. D. Wu. "Personalized Steering Feel Design for Steer-by-Wire Systems Based on the Rack Force Estimation." ;,Proc., *International Journal of Automotive Technology* 24, no. 4 (Aug 2023): 1151-61.

He, L., F. L. Li, C. L. Guo, B. Z. Gao, J. B. Lu, and Q. Shi. "An Adaptive Pi Controller by Particle Swarm Optimization for Angle Tracking of Steer-by-Wire."; ,Proc., *Ieee-Asme Transactions on Mechatronics* 27, no. 5 (Oct 2022): 3830-40.

Jin W.L. " Research on Chassis Domain Control Strategy for Intelligent Vehicles Based on Sensor Analytical Redundancy , " M.S. Thesis, *Jilin University*, Changchun, Jilin. (2022)

Li C, Wang Y, Wang X, et al. "Differential steering control strategy of distributed hybrid all-terrain vehicles based on improved genetic algorithm optimization";,Proc.,*2022 IEEE 10th Joint International Information Technology and Artificial Intelligence Conference (ITAIC). IEEE*. 10, 01-06 (2022)

Liu S, Zhu Y Q, Ji X W. "Research on Design of Variable Gear Ratio of Steer-by-Wire System and Comprehensive Feedback Control of Front Wheel Angle,"; ,Proc.,*2021 China Automation Congress (CAC). IEEE*. 1898-1903 (2021)

Mezura-Montes, E., and C. A. C. Coello. "Constraint-Handling in Nature-Inspired Numerical Optimization: Past, Present and Future," . *Swarm and Evolutionary Computation* 1, no. 4 (Dec 2011): 173-94.

Pietruch, M., A. Wetula, and A. Mlyniec. "Influence of the Accuracy and Can Frame Period of the Steering Wheel Angle Sensor (Sas) on the Trajectory of a Steer-by-Wire-Equipped Car,";,Proc., *Ieee Access* 10 (2022): 106110-16.

Shi J, XU Guang, J. "Realization of Steering Road Simulation in ADAS Experimental Platform,". *Mechanical Design & Manufacturing*. (5), 29-32 (2022)

Shi, Q., Y. J. Wei, D. Xie, F. L. Li, K. Song, and L. He. "A Model Predictive Control Approach for Angle Tracking of Steer-by-Wire System with Nonlinear Transmission Ratio.". *Asian Journal of Control* 25, no. 2 (Mar 2023): 1156-66.

Sun, Z., J. C. Zheng, and Z. H. Man. "Adaptive Sliding Mode Control for a Vehicle Steer-by-Wire System,";,Proc., *Proceedings of 2016 2nd International Conference on Control Science and Systems Engineering (Iccsse)* (2016): 77-81.

Wei, H. Y.et al. "Steer-by-Wire Control System Based on Carsim and Simulink,"; ,Proc., *2021 Ieee International Iot, Electronics and Mechatronics Conference (Iemtronics)* (2021): 941-45.

Xie L G, chen Y, Guo X G." Research on active steering control of wired steering system vehicles,". *Mechanical design and manufacturing*. 1-8, 1001-3997 (2023)

XIE L G, Chen Y. "Road feel control strategy of steer-by-wire vehicle,". *Journal of Chongqing University of Technology (Natural Science)*. 36(4), 68-74 (2022)

Xu, F. X., X. H. Liu, W. Chen, C. Zhou, and B. W. Cao. "Fractional Order Pid Control for Steer-by-Wire System of Emergency Rescue Vehicle Based on Genetic Algorithm,". *Journal of Central South University* 26, no. 9 (Sep 2019): 2340-53.

Xu Z. A , et al. "A Generalized Predictive Control Approach for Angle Tracking of Steer-by-Wire System,"; ,Proc., *Proceedings of the 61th Annual Conference of the Society of Instrument and Control Engineers of Japan (SICE)*, Tokyo, Japan. 8-10 September 2022

Yin F Q. "Research on ideal transmission ratio and front wheel angle control strategy of steer by wire system,". M.S. Thesis, *Changan University*, Xian, Shanxi (2019)

Yu, Z. P. Yu Y., Yang X., et al. "Steering Angle Control of Sbw System Based on Internal Model Control,"; ,Proc., *Proceedings of the 33rd Chinese Control and Decision Conference (Ccdc 2021)* (2021): 1881-86.

Zhang, G. W., X. Y. Wang, L. Li, and W. B. Shao. "Design and Applications of Steering Angle Tracking Control with Robust Compensator for Steer-by-Wire System of Intelligent Vehicle,". *Ifac Papersonline* 54, no. 10 (2021): 221-27.

Zhang, X. H., L. H. Zhao, G. H. Ji, and Z. Y. Liu. "Angle Tracking Control Strategy for Steering-by-Wire System with Dual Steering Actuator Motors."; ,Proc., *2022 41st Chinese Control Conference (Ccc)* (2022): 5359-64.

Zhang, L., Z. H. Wang, X. L. Ding, S. H. Li, and Z. P. Wang. "Fault-Tolerant Control for Intelligent Electrified Vehicles against Front Wheel Steering Angle Sensor Faults During Trajectory

Tracking,"; ,Proc.,*Ieee Access* 9 (2021): 65174-86.

線控轉向系統角度跟蹤的自我調整分數階 PID 控制器

郭聰聰　吳長水
上海工程技術大學機械與汽車工程學院
何德管
蘇州衡魯汽車部件有限公司

摘 要

為了保證汽車轉向過程中快速準確的角度跟蹤，減少延遲時間，提高線控轉向系統的跟蹤性能，設計了一種具有前饋補償的分數階 PID 控制器。PID 控制器採用 Oustaloup 近似方法進行近似，減小了 FOPID 的整定維數。利用改進的粒子群優化演算法對 FOPID 的四個參數進行動態調整，從而縮短了演算法的優化時間。最後，將基於全域搜索模式的自我調整慣性權重粒子群優化演算法（AW-PSO）、基於可變鄰域搜索模式的固定慣性權重粒子團優化演算法（F-PSO）和壓縮因數粒子群優化方法（CF-PSO）進行了模擬驗證和台架試驗。驗證了該方法的有效性。比較結果表明，在計算時間和精度方面，該方法的優化能力明顯優於 AW-PSO、F-PSO 和 CF-PSO 演算法。因此，該演算法的計算精度和穩定性完全滿足要求。台架試驗結果表明，在階躍輸入下，延遲時間約為 0.2s，最大過衝量為 1.57deg。在正弦輸入下，延時時間約為 0.02s，最大轉向速度為 0.70rad/s，轉向電機的最大輸出扭矩為 2.27Nm。基於實驗驗證，可以得出這樣的結論：該方法能夠更好地完成 SBW 系統的角度跟蹤控制任務，並表現出良好的魯棒性和跟蹤控制性能